

# High Temperature ( $>200^{\circ}\text{C}$ ) Isolated Gate Drive Topologies for Silicon Carbide (SiC) JFET

S. Waffler, S.D. Round and J.W. Kolar  
Power Electronic Systems Laboratory  
ETH Zurich  
8092 Zurich, Switzerland  
Email: waffler@lem.ee.ethz.ch

**Abstract**—Volume and weight limitations for components in hybrid electrical vehicle (HEV) propulsion systems demand highly-compact and highly-efficient power electronics. The application of Silicon Carbide (SiC) semiconductor technology in conjunction with high temperature (HT) operation allows the power density of the DC-DC converters and inverters to be increased. Elevated ambient temperatures of above  $200^{\circ}\text{C}$  also affects the gate drives attached to the power semiconductors. This paper focuses on the selection of HT components and discusses different gate drive topologies for SiC JFETs with respect to HT operation capability, limitations, dynamic performance and circuit complexity. An experimental performance comparison of edge-triggered and phase-difference HT drivers with a conventional room temperature JFET gate driver is given. The proposed edge-triggered gate driver offers high switching speeds and a cost effective implementation. Switching tests at  $200^{\circ}\text{C}$  approve an excellent performance at high temperature and a low temperature drift of the driver output voltage.

## I. INTRODUCTION

High temperatures in the propulsion system of Hybrid Electrical Vehicles (HEV) provide a harsh environment for power electronic systems such as DC-DC converters and inverters. The same environmental conditions also apply for military, space exploration or energy exploration applications [1] and demand High Temperature (HT) capable electronics. Silicon Carbide (SiC) semiconductors are especially valuable in these fields of application due to the SiC material properties.

In comparison to silicon, SiC has a larger band gap and thus allows higher junction temperature operation, which minimizes heat sink volume or provides the possibility to integrate the power electronics with the engine and the engine coolant of a HEV [2]. The higher saturated electron drift speed increases switching speed [1] and thus allows a reduction of the size and weight of the converter's passive components.

The only available SiC switch is the normally-on JFET that offers larger forward current ratings and lower on resistance [3], whereas normally-off devices like SiC-BJT, SiC-MOSFETs and IGBTs are being researched by semiconductor manufacturers for future application.

Since it is necessary to place the gate drive physically close to a SiC-JFET, operation at elevated ambient temperature of above  $200^{\circ}\text{C}$  is required and a switching frequency of approximately 250kHz is desired to benefit from the SiC dynamic properties. Furthermore, for a DC-DC converter application a

large duty range is essential and the capability to statically turn off the normally-on device is required for protection reasons.

A typical JFET gate drive circuit for room temperature operation that provides these requirements is shown in Fig. 1. A digital isolator  $IC1$  is applied to electrically isolate the PWM signal from the high voltage and feeds a subsequent integrated driver circuit  $IC2$  that generates the JFET gate voltage  $u_{gs}$ .  $IC1$  and  $IC2$  are connected to a transformer-isolated auxiliary power supply. Circuit extensions can provide better switching performance [4] or protection functionality [5].

The optical or integrated magnetic couplers that are typically utilized for  $IC1$  as well as the integrated circuit  $IC2$  are not operable at high temperature because of aging effects and/or other material limitations like maximum junction temperature. Only a small number of components fulfills the requirements for operating temperature range.

Therefore, high temperature operation of gate drivers that also have high performance poses a significant challenge in both component and topology selection. Section II of this paper deals with materials and components for HT operation. Different drive topologies that utilize this component portfolio are evaluated in Section III. Comparative experimental results for the selected drive topologies are presented in Section IV.

## II. COMPONENT SELECTION

### A. Passive components

HT resistors are standard components with the maximum allowable power dissipation as the limiting factor. Since power dissipation decreases with temperature, resistors with higher power rating must be chosen. The influence of the temperature coefficient (TC) is considerably low for a gate drive application.

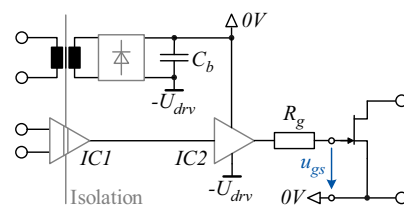


Fig. 1. Typical gate driver design using an isolated power supply, a digital isolator  $IC1$  and an integrated driving circuit  $IC2$ .

This is different for capacitors where the temperature characteristics of ceramic dielectrics like X7R or Y5U are very unstable [6] and induce a capacitance drop of 50% or more at the desired temperature. The selected HT SMT capacitors by Advanced Monolithic Capacitors (AMC) with temperature stable NPO dielectric are rated for 200°C.

Furthermore, suitable magnetic materials are required for the isolating transformers. The maximum operation temperature for coated powder, ferrite or strip-wound cores is in the range of 125 - 200°C [7] because of the epoxy coating. That is why uncoated toroidal ferrite cores with high Curie temperature  $T_c$  are preferred. The transformers used for the gate drivers are constructed from Magentics L material [8] cores, which have a  $T_c > 300^\circ\text{C}$  and relatively good magnetic and core loss characteristics, and the windings are made with Polyamidimid coated grade 2 magnet wire. An alternative is to avoid magnetic materials by the application of coreless transformers.

### B. Active components

Increasing substrate leakage currents limit the maximum allowable junction temperature for silicon integrated circuits. Alternatives for HT active components are SiC or Silicon On Insulator (SOI) technology that provide significant reliability and performance advantages.

There is a wide variety of SiC diodes, also for low power applications like a HT gate drive but on the contrary, no discrete small signal transistors or integrated circuits.

However, a very restricted assortment of SOI products is available. This includes operational amplifiers, gate logic and discrete components. A promising part for the HT gate driver is a 1A SOI MOSFET by Honeywell (HTNFET).

### C. Mechanical

From a mechanical point of view, there are two major concerns. These are the HT substrate and the packaging of the active components.

Firstly, epoxy resins are characterized by their glass transition temperature  $T_g$  above which the material becomes soft. This is one of the reasons why ceramic substrates like  $\text{Al}_2\text{O}_3$  or  $\text{AlN}$  are preferred to standard FR-4 ( $T_g \approx 130^\circ\text{C}$ ) or High-Tg FR-4 ( $T_g \approx 170^\circ\text{C}$ ). A further reliability-related material property is the coefficient of thermal expansion (CTE). The CTE of the base material should be similar to that of the conductor material otherwise unequal expansion of substrate and conductor will crack tracks or vias. The FR-4 materials show a large CTE in z-direction and can not be used.

However, there are special laminates like Arlon 85N, Isola IS410 or Rogers RO4530B that can be handled with a cost-saving standard PCB process and provide high  $T_g$  and low CTE at the same time such as  $T_g > 280^\circ\text{C}$  and  $\text{CTE}(z) = 35\text{ppm}/^\circ\text{C}$  for the selected RO4530B substrate.

Secondly, as conventional epoxy packages do not withstand the temperature, usually a Multi-Chip Power Module (MCPM) is the packaging technique of choice. As a matter of costs and handling, HT MOSFETs in a HT ceramic package and

SiC components in standard packages are to be placed on RO4530B substrate in a first step.

## III. TOPOLOGY EVALUATION

For a cost-optimized gate driver design the number of HT components, especially of non-standard active components like MOSFETs needs to be minimized. Purely passive drives, simple active drives and more advanced active drives are evaluated in respect to their suitability for application to SiC JFETs employed in DC-DC converters.

### A. Transformer Coupled Gate Drive Circuits

A simple gate driver with an isolation transformer but without active components is depicted in Fig. 2 (a). Since the volt seconds product of positive and negative half-wave of the transformer secondary voltage  $u_{gs}$  are forced to be equal, the circuit output is bipolar.

The bipolar signal is the cause of two problems, firstly, at low duty cycles the amplitude of the negative half-wave drops and will turn on the JFET when  $u_{gs}$  exceeds the threshold voltage  $U_{th}$ . Secondly, the positive JFET gate voltage should be kept below the threshold of the gate junction to avoid its destruction when no further current limitation is provided.

An additional capacitor  $C_c$  and a diode  $D_c$  extends the circuit to the DC Restore Circuit (Fig. 2 (b)) with output voltage either 0V or  $u_{p,pk-pk}$  for a turns ratio of 1:1.

A constant voltage at the transformer primary saturates the core. To prevent saturation, a PWM signal  $u_p(t)$  must be applied. Unfortunately, this fact disqualifies both circuits since the normally-on JFET cannot be turned off permanently.

### B. High-Frequency Carrier

To overcome the drawback of the above circuits and to provide the possibility of a permanent JFET turn-off, a high frequency (HF) carrier could be modulated with the PWM signal. In order to turn the JFET off, the HF carrier is applied to the primary of a isolating transformer  $T_1$  and rectified at its secondary side to provide a negative gate bias at  $C_1$  (Fig. 3).

Whereas  $C_1$  is charged quickly after the HF carrier is applied,  $C_1$  has to be discharged by  $R_1$  to turn the JFET on,

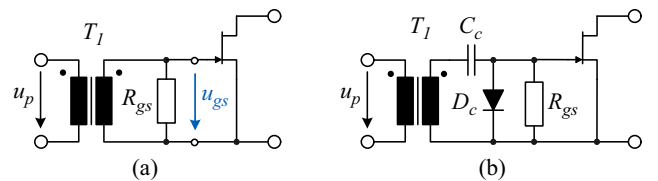


Fig. 2. Transformer Coupled circuits: (a) Simple, (b) DC Restore Circuit

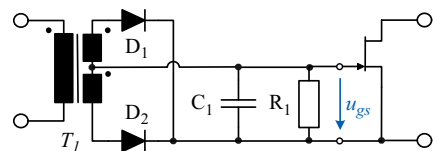


Fig. 3. High-Frequency Carrier Circuit

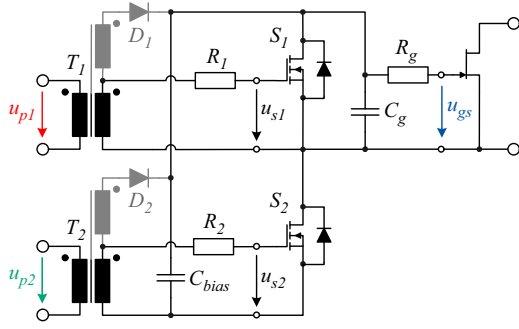


Fig. 4. Phase-Difference Circuit

which significantly decreases the switching speed. Therefore, additional circuitry is required to actively discharge  $C_1$ .

A HF carrier gate driver with a resonantly operated coreless transformer (CT) is proposed in [9]. It has been determined by using simulation and measurements that the additional time to build up a steady oscillation at the CT secondary is too long to achieve short rise and fall times of  $u_{gs}$  and therefore high switching frequency operation.

Furthermore, it should be noted that the rectification of a very high frequency carrier signal with HT SiC diodes is poor since the available power diodes have large junction capacitances.

### C. Phase-Difference Circuit

In order to provide continuous negative gate bias for the JFET, to overcome the duty-cycle limitations that are unavoidable with passive driving circuits and to achieve high switching speeds at the same time, actively controllable switches like MOSFETs are required in the gate driver.

A basic principle that also applies to integrated gate drivers is to use a storage capacitor  $C_{bias}$  in connection to a half-bridge structure  $S_1, S_2$  connected to the JFET gate (Fig. 4). By applying appropriate control signals to the gates of the two half-bridge switches either zero volts or the bias capacitor voltage  $U_{bias}$  is switched to the JFET gate.

When isolation of the control signals  $u_{gs1}$  and  $u_{gs2}$  is provided by transformers  $T_1$  and  $T_2$  the problem of the duty cycle limitation existing with passive drivers is shifted to the auxiliary switches  $S_1$  and  $S_2$ . For an assumed 50% duty cycle that means if  $u_{p1}$  is switching and  $u_{p2} = 0$  the half bridge output is changing between  $U_{bias}$  ( $S_1$  on) and high impedance ( $S_2$  off) and in case that  $u_{p1} = 0$  and  $u_{p2}$  is switching the half-bridge output is changing between  $0V$  and high impedance. The actual JFET gate voltage  $u_{gs}$  is preserved during the high impedance state due to the JFET input capacitance and an optional external capacitor  $C_g$  as indicated in Fig. 5. By continuous pulsing of  $S_2$  the circuit is able to generate a static negative gate voltage at the JFET and thus turn the JFET off permanently. Due to the method of operation the drive concept is known as a Phase-Difference Drive [10].

The bias capacitor  $C_{bias}$  itself is charged by rectification of the carrier signals  $u_{p1}$  or  $u_{p2}$  with the diodes  $D_1$  or  $D_2$ .

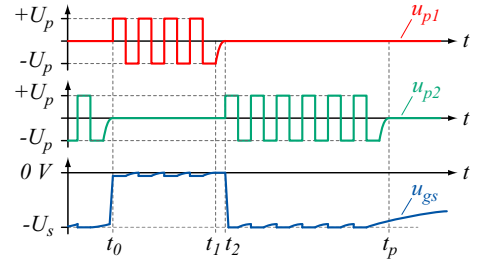


Fig. 5. Timing diagram for Phase Difference Circuit: Either switch  $S_1$  or  $S_2$  are switched to connect  $C_{bias}$  or  $0V$  to the output respectively.

In conclusion, the circuit provides unlimited off-time, has no duty cycle limitation and fast switching transients of the JFET because of the active components  $S_1$  and  $S_2$ .

### D. Bootstrap Power Supply

To drive a JFET bridge leg, a novel Bootstrap Power Supply concept is proposed for the Phase Difference Driver to simplify the bias voltage generation. Taking the negative output voltage into account, the bootstrap diodes  $D_{bst}$  for the high-side JFET driver needs to be connected to a voltage source  $U_P$  referenced to the positive DC supply rail and charge the bootstrap capacitors  $C_{bst}$ . The capacitors  $C_{bias}$  of the low-side JFET drives are connected to a voltage source  $U_N$  referenced to the negative DC supply rail.

### E. Edge-Triggered Circuit

A driving circuit of less complexity that provides the same functionality as the Phase-Difference Circuit is the proposed Edge-Triggered Drive Circuit depicted in Fig. 7. The circuit basically consists of a single pulse transformer  $T_1$ , an auxiliary MOSFET switch  $S_1$ , the diode  $D_2$  and the capacitor  $C_g$  and

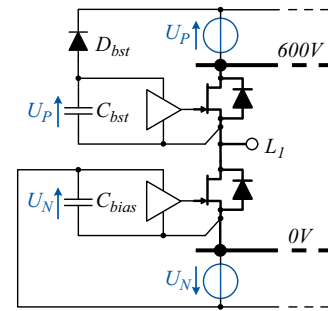


Fig. 6. Bootstrap Power Supply for the Phase Difference Driver

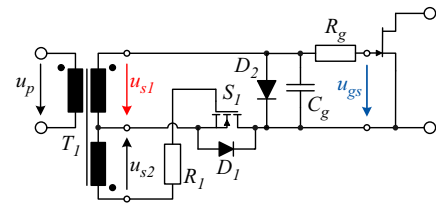


Fig. 7. Edge-Triggered Circuit

thus only needs half the components compared to the Phase-Difference drive without loss of performance as will be shown in Section IV.

The number of turns on the secondary winding 1 is selected to achieve a peak output voltage  $U_{s1}$  of at least the JFET threshold voltage  $U_{th}$  and the number of turns on the secondary winding 2 to provide an appropriate gate voltage to  $S_1$ .

To turn the JFET off, a short negative voltage pulse of width  $T_{PW}$  is applied to the transformer primary. In this case  $S_1$  is turned off because of the negative gate voltage  $u_{s2}$ . The secondary voltage  $u_{s1}$  causes  $D_2$  to block,  $D_1$  conducts and  $C_g$  is charged to  $-U_{s1} < U_{th}$  (Fig. 8 (b)). At the end of the pulse ( $u_p = u_{s1} = u_{s2} = 0V$ )  $S_1$  turns off, isolates the JFET from the pulse transformer and thus prevents  $C_g$  discharging through the transformer secondary winding (Fig. 8 (c)). Continuous negative pulses can be used to permanently turn off the JFET like depicted in Fig. 9 for  $t_a < t < t_0$ .

To turn the JFET on, a positive pulse of width  $T_{PW}$  is applied to the transformer primary. Since  $u_{s2} > 0$ ,  $S_1$  is turned on and  $C_g$  is discharged. The positive voltage is clamped by  $D_2$  so that the circuit output voltage is  $u_{gs} = 0V$  (Fig. 8 (a)).

For high-speed operation care must be taken with the selection of the components. The capacitance of  $C_g$  is a critical parameter because large values increase the rise and fall time of the drive output voltage. On the other hand, the output capacitance  $C_{oss1}$  of  $S_1$  must be taken into account: Once the voltage  $u_{p1}$  returns to zero after a negative pulse that previously turned off the JFET, charge is drawn from  $C_g$  in order to charge  $C_{oss1}$  (Fig. 8 (c)). Therefore, low  $C_g$  values would cause an unintentional drop of the drive output voltage.

The short pulse width  $T_{PW}$  is a further advantage that results in a low volt seconds product for the transformer and thus a minimal transformer core size. This is important for minimal transformer parasitics like leakage inductance  $L_\sigma$  and primary to secondary coupling capacitance  $C_c$ . Small  $L_\sigma$  leads to high switching speeds and a small  $C_c$  ensures low common-mode currents resulting from the high  $dv/dt$  levels of the JFET Drain-Source voltage  $u_{ds}$ .

Furthermore, it should be noted that in practice a voltage overshoot  $U_{ov}$  (Fig. 15) at turn-off of the JFET is observed due to the resonant circuit formed by the secondary-side leakage inductance  $L_\sigma$  of the transformer  $T_1$  and the storage capacitor  $C_g$ . This behavior also has a positive effect on the switching speed as will be shown later on.

#### IV. EXPERIMENTAL RESULTS

As purely passive drivers or DC restore circuits cannot turn off the JFET permanently and the HF carrier circuits lack switching performance, the Phase-Difference and Edge-Triggered drivers are considered as candidate topologies in spite of the higher component effort.

For further investigation different versions of these two circuits and a standard low temperature gate driver (Fig. 1) were built and tested by switching an inductive load  $L$  with a SiCED SiC JFET (1300V, 4A,  $U_{th} = -25V$ ) and a

Cree CSD10060 SiC Schottky diode (1200V, 10A) that are connected to a DC link capacitor  $C_{DC}$  (Fig. 10).

#### A. Topology Comparison

For a first performance comparison, the different drivers were built with standard components and operated at room temperature. To ensure identical measurement conditions, each gate drive topology is routed on a separate interchangeable PCB. Furthermore, the transformers  $T_1$  and  $T_2$  of the Phase-Difference Circuit and  $T_1$  of the Edge-Triggered Circuit share the same core and winding geometry. Gate resistors of  $R_g = 10\Omega$ , Cree SiC diodes CSD04060 in a TO-252-2 package and Zetex ZVN4206G MOSFETs with gate resistors of  $R_1 = R_2 = 47\Omega$  are used in each topology. The PWM and different drive control signals are generated by a DSP and a FPGA.

$IC1$  and  $IC2$  of the Standard Drive are an Analog Devices ADuM1100BR magnetic coupler and an IXYS IXDN404SI MOSFET driver respectively. A capacitor  $C_g = 2.2nF$  is utilized in the Edge-Triggered Circuit as a compromise between switching speed, gate drive losses and the voltage drop in  $u_{gs}$  that is encountered when  $C_{oss1}$  is charged. A pulse width  $T_{PW}$  of 130ns was found to be the minimum value to transfer the necessary gate charge. The carrier frequency for the Phase Difference Drive is set to 1MHz with a dead time of 250ns when switching between the two carrier signals  $u_{p1}$  and  $u_{p2}$  to prevent a short circuit of the half-bridge  $S_1$ ,  $S_2$  and oscillations in the drive output  $u_{gs}$ . The transformers of Phase Difference and Edge-Triggered Circuit are interfaced to the PWM FPGA by IXYS IXDN404SI driver ICs.

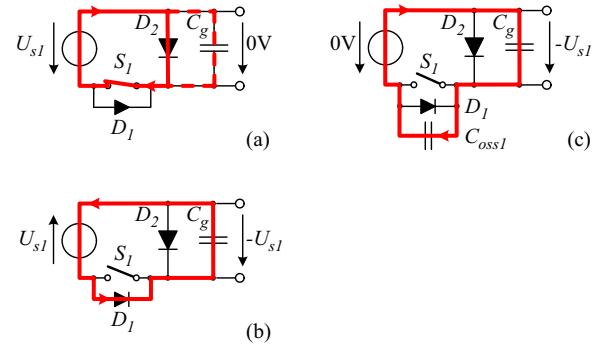


Fig. 8. Modes of Operation of edge-triggered drive circuit: (a) positive voltage pulse applied to the transformer primary, (b) negative voltage pulse applied, (c) no voltage applied to the transformer primary.

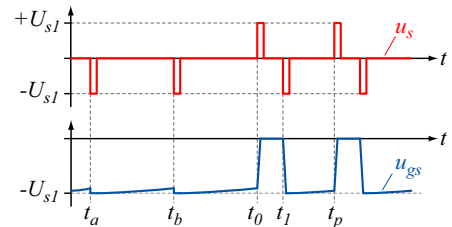


Fig. 9. Timing diagram for Edge-Triggered Circuit: Short pulses are applied to charge or discharge the output capacitor  $C_g$ .

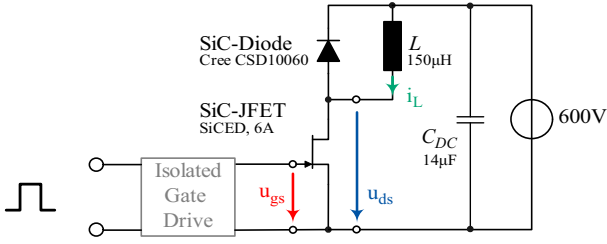


Fig. 10. Test setup with gate drive and power stage consisting of a SiC JFET, a SiC diode, DC-link capacitor  $C_{DC}$  and inductor  $L$ .

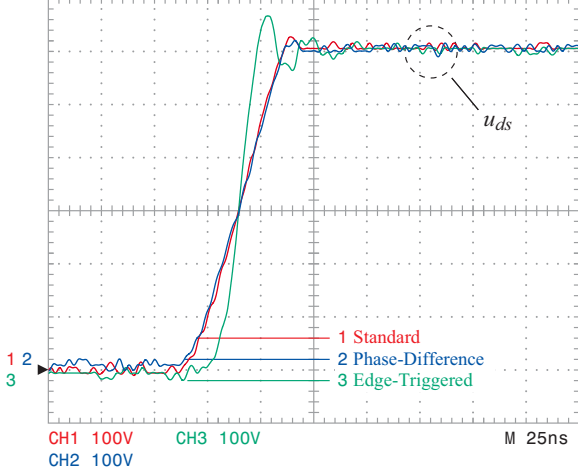


Fig. 11. Comparison of the JFET Drain-Source voltage  $u_{ds}$  rise times (JFET turn-off) for different driver topologies at room temperature.

The inductive load  $L$  is constructed using three E30 cores, each with a single layer winding to minimize the parasitic capacitance and  $C_{DC}$  consists of four  $3.3\mu\text{F}$  film capacitors in parallel with two  $220\text{nF}$  HV ceramic capacitors.

For each driver a switching cycle with  $i_L = 5\text{A}$  at turn-on of the JFET to  $i_L = 6\text{A}$  at turn-off (Fig. 14) was initiated at a DC link voltage of  $600\text{V}$ . The fall time  $t_f$  and rise time  $t_r$  (Fig. 11) measurements of the drain source voltage  $u_{ds}$  show no drop in switching performance for the two HT topologies. On the contrary, the resonant voltage overshoot  $U_{ov}$  (Fig. 15) of  $u_{gs}$  for the Edge-Triggered Driver improves the voltage slopes.

The resulting rise and fall times are listed in Table I. With the Edge-Triggered Driver, which performed best in the comparison, maximum  $dv/dt$  levels of  $-60.0\text{kV}/\mu\text{s}$  at turn-on and  $38.1\text{kV}/\mu\text{s}$  at turn-off are achieved. Therefore, high JFET switching frequencies of  $250\text{kHz}$  and above are feasible.

TABLE I  
SiC JFET SWITCHING TIMES AT ROOM TEMPERATURE

Topology	Turn on		Turn off	
	$t_f$ (ns)	Slope (kV/ $\mu\text{s}$ )	$t_r$ (ns)	Slope (kV/ $\mu\text{s}$ )
Standard	17.7	-34.4	35.4	17.2
Phase-Difference	18.4	-32.0	34.9	17.2
Edge-Triggered	10.2	-60.0	16.3	38.1

## B. $dv/dt$ Immunity

High  $dv/dt$  levels of the JFET Drain-Source voltage result in a common mode current through the parasitic coupling capacitance  $C_c$  of the electrical isolators of a gate drive. A robust gate drive should provide a good immunity to this current and therefore a low  $C_c$ . The transformers for the presented drives (15:15:7 turns on a R9.5 toroid) have a  $C_c$  of  $12\text{pF}$ . The common mode rejection of the Edge-Triggered drive is verified with a switched voltage ( $600\text{V}$ ,  $dv/dt = -60\text{kV}/\mu\text{s}$ ) that is applied between the shorted primary winding of  $T_1$  and the source connector at the output of the drive.

A disturbance of no more than  $50\text{mV}$  is measured at the drive output voltage during the switching instants during non-switching of the driver ( $S_1$  is blocking,  $C_c$  connected in series with  $C_{oss1}$ ). Further measurements during the time a control pulse is applied to the transformer primary ( $S_1$  is conducting) will be conducted.

## C. High Temperature Operation

Due to the promising performance of the Edge-Triggered Driver at room temperature the circuit was built with HT components, including the transformer  $T_1$  (Magnetics L material, HT wire),  $S_1$  (Honeywell HTNFET),  $D_1$  (SiC diode Cree CSD04060, standard package),  $C_g$  (AMC NPO capacitors) and HT resistors (Fig. 12). The components are assembled on RO4530B substrate with HMP solder. The resistors  $R_p$ ,  $R_{s1}$  and a suppressor diode were added for protection of the HTNFET, but are not required for nominal operation.

The driver PCB is plugged onto a test circuit according to Fig. 10 that was built with X7R HV ceramic capacitors  $C_{DC}$  and a inductive load  $L$  made of an air-gapped Metglas AMCC 25 core and silicon wire and is operated inside a heating oven as shown in Fig. 13. An FPGA outside the oven and IXYS driver ICs that are enclosed inside a box and cooled with air from outside the oven generate the control pulses.

The operation of the driver was verified with switching cycles as shown in Fig. 14 for a temperature of  $200^\circ\text{C}$ . At  $200^\circ\text{C}$  and a load current of  $i_L = 6\text{A}$  the measured  $u_{ds}$  rise and fall times were  $t_r = 10.7\text{ns}$  and  $t_f = 14.3\text{ns}$  according to  $dv/dt$  levels of  $-57.1\text{kV}/\mu\text{s}$  and  $41.7\text{kV}/\mu\text{s}$ .

As shown in Fig. 15, no significant change in the switching characteristics is observed when the temperature is raised to  $200^\circ\text{C}$ . However, due to the temperature dependence of the semiconductor parameters, a minor drop of the gate driver

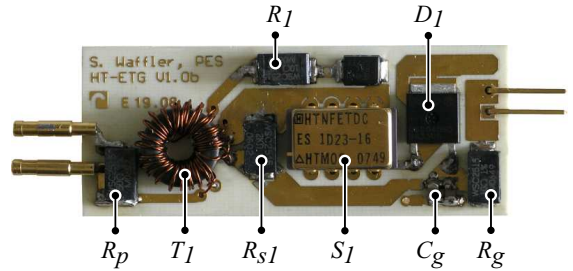


Fig. 12. Prototype PCB of the  $200^\circ\text{C}$  Edge-Triggered Driver

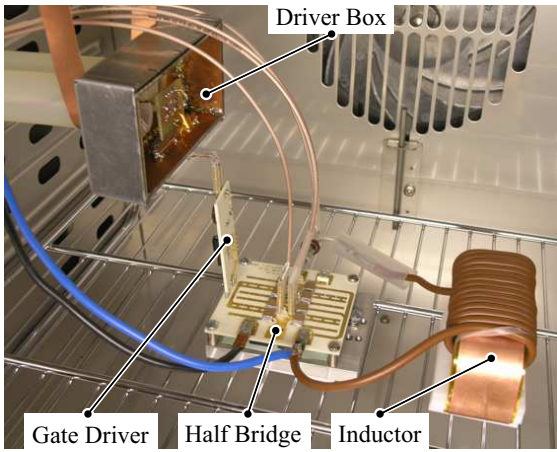


Fig. 13. Test setup inside the heating oven for inductive load switching tests

output voltage from  $-25.1\text{V}$  at room temperature to  $-23.8\text{V}$  at  $200^\circ\text{C}$  is observed, equivalent to a low temperature drift of  $7.4\text{mV/K}$  for the driver circuit.

## V. CONCLUSION

In this paper different SiC JFET gate drive topologies for use in a SiC DC/DC converter and High Temperature (HT) operation are evaluated. The candidate drive circuits are selected considering the aspects of HT component availability and costs, gate drive performance and additional requirements like the ability to permanently turn off a normally-on JFET. Furthermore, the passive and active HT components as well as the magnetic and substrate materials for the construction of these drives are investigated.

A Phase Difference Driver and the proposed Edge-Triggered Driver are compared experimentally with a conventional room temperature driver in regard to performance whereas the Edge-Triggered Driver shows excellent switching speeds and a cost-effective design due to a minimal HT component count.

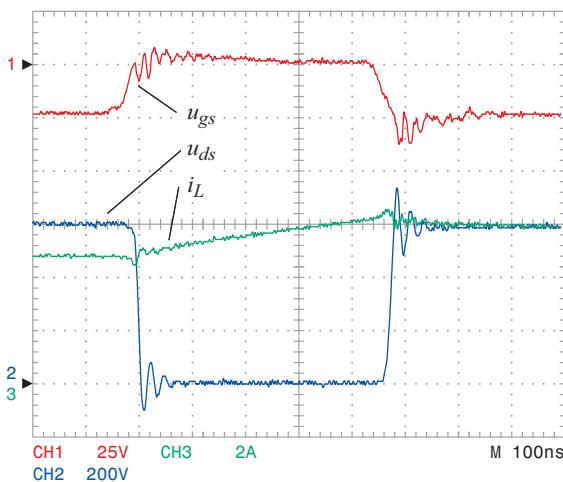


Fig. 14. Switching cycle for the High-Temperature Edge-Triggered Driver at  $200^\circ\text{C}$  and  $U_{DC} = 600\text{V}$ ,  $5\text{A} < i_L < 6\text{A}$

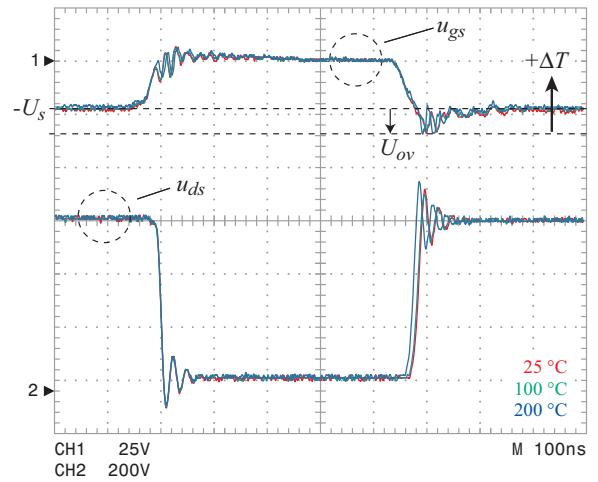


Fig. 15. Temperature dependence of Edge-Triggered circuit output voltage  $u_{gs}$  (resonant voltage overshoot  $U_{ov}$ ) and the JFET drain source voltage  $u_{ds}$ .

The HT operation of the proposed Edge-Triggered Driver is verified by switching tests at a maximum temperature of  $200^\circ\text{C}$  without a drop in the switching performance. The maximum measured  $dv/dt$  levels of the JFET Drain-Source voltage of  $-57.1\text{kV}/\mu\text{s}$  and  $+41.7\text{kV}/\mu\text{s}$  demonstrate a very high performance of the HT Edge-Triggered Driver and the usability for high switching frequencies above  $250\text{kHz}$ . Furthermore, the driver output voltage shows a low temperature drift of only  $7.4\text{mV/K}$ .

## REFERENCES

- [1] J. Hornberger, A.B. Lostetter, K.J. Olejniczak, T. McNutt, S.M. Lal, and A. Mantooth, "Silicon-Carbide (SiC) Semiconductor Power Electronics for Extreme High-Temperature Environments," in *IEEE Aerospace Conference*, vol. 4, Mar. 2004, pp. 2538–2555.
- [2] F. Renken, G. Ehbauer, V. Karrer, R. Knorr, S. Ramminger, N. Seliger, and E. Wolfgang, "Reliability of High Temperature Inverters for HEV," in *Power Conversion Conference 2007*, Apr. 2007, pp. 563–568.
- [3] R. Kelley and M.S. Mazzola, "SiC JFET Gate Driver Design for Use in DC/DC Converters," in *Applied Power Electronics Conference (APEC 2006)*, Mar. 2006, pp. 179–182.
- [4] S. Round, M. Heldwein, J.W. Kolar, I. Hofsjager, and P. Friedrichs, "A SiC JFET Driver for a 5 kW, 150 kHz Three-Phase PWM Converter," in *Industry Applications Society Annual Meeting 2005*, vol. 1, Oct. 2004, pp. 410–416.
- [5] A. Orellana and B. Piebenbreier, "Fast Gate Drive for SiC-JFET using a Conventional Driver for MOSFET and Additional Protections," in *30th annual Conference of IEEE (IECON)*, vol. 1, Nov. 2004, pp. 938–943.
- [6] E. Cilio, J. Garrett, J. Fraley, B. McPherson, J. Hornberger, M. Schupbach, and A. Lostetter, "High Temperature Electronics ( $>485^\circ\text{C}$ ) For Venus Exploration," in *4th International Planetary Probe Workshop*, Pasadena, California, Jun. 2006.
- [7] M. Swihart, "Designing High Temperature Magnetics," in *47th European Power Electronics Conference (PCIM)*, May 2003, pp. 223–228.
- [8] R. Spyker, J. Huth, I. Mehdi, and A. Brockschmidt, "300C ferrite material for high temperature magnetics," in *Power Electronics Specialists Conference (PESC)*, Jun. 2004, pp. 155–160.
- [9] S.Y. Hui, S.C. Tang, and H. Chung, "Optimal Operation of Coreless PCB Transformer-Isolated Gate Drive Circuits with Wide Switching Frequency Range," *IEEE Trans. Power Electron.*, vol. 14, no. 3, pp. 506–514, May 1999.
- [10] D. C. Hopkins, D. W. Kellerman, R. A. Wunderlich, C. Basaran, and J. Gomez, "High-temperature, high-density packaging of a 60kW converter for  $>200^\circ\text{C}$  embedded operation," in *Applied Power Electronics Conference (APEC)*, Mar. 2006, pp. 871–877.